

Electronic Supplementary Information

Hybrid Networks Constructed from Tetrahedral Silicon-Centered Precursors and Cubic POSS-Based Building Blocks via Heck Reaction: Porosity, Gas Sorption, and Luminescence

Dengxu Wang,^{a,b} Wenyan Yang,^a Ligu Li,^a Xian Zhao,^b Shengyu Feng,^{*a} and Hongzhi Liu^{*a}

^aKey Laboratory of Special Functional Aggregated Materials, Ministry of Education, School of Chemistry and Chemical Engineering, Shandong University, Jinan 250100, P. R. China

^bState Key Lab of Crystal Materials, Shandong University, Jinan 250100, P. R. China

*Corresponding Author. Tel: +86 531 88364866. Fax: +86 531 88564464. E-mail: fsy@sdu.edu.cn; liuhongzhi@sdu.edu.cn

Table of contents:

Fig. S1. Energy dispersive spectroscopy of HPP-1 to HPP-5

Fig. S2. FT-IR spectrum of HPP-1 to HPP-5

Fig. S3. Solid-state ^{13}C CP/MAS NMR spectra of HPP-1~HPP-5 at an expanded scale from 100 ppm to 160 ppm

Fig. S4. Nitrogen sorption isotherms of HPP-1 (a) and (b) HPP-2. Filled and empty symbols denote adsorption and desorption branches. The porosity data of HPP-1: $S_{\text{BET}} = 167 \text{ m}^2 \text{ g}^{-1}$, $V_{\text{total}} = 0.18 \text{ cm}^3 \text{ g}^{-1}$.

Fig. S5. BET plots of HPP-3 (up, $r = 0.999958$, $C = 290.91$), HPP-4 (middle, $r = 0.999956$, $C = 299.075$) and HPP-5 (bottom, $r = 0.999927$, $C = 298.54$)

Fig. S6. TGA curves of OVS and HPP-1~HPP-5 under N_2 ($10 \text{ }^\circ\text{C min}^{-1}$)

Fig. S7. The XRD pattern of HPP-1 to HPP-5

Fig. S8. FE-SEM images of a) HPP-4 and b) HPP-5

Fig. S9. Gas sorption isotherms of HPP-5. (a) H_2 adsorption isotherm at 77 K. (b) CO_2 adsorption and desorption isotherm, and CH_4 adsorption isotherm at 298 K. Filled and empty symbols denote adsorption and desorption branches, respectively.

Fig. S10. (a) H_2 adsorption isotherm of HPP-5 at 87 K; (b) Isothermic heats of sorption for H_2 on HPP-5.

Fig. S11. Toth model fitting of CO_2 (a) and CH_4 (b) adsorption isotherms of HPP-5 at 298 K

Fig. S12. Fluorescent spectra of monomers, **1~5** in the solid state (excited at 310 nm)

Fig. S13. Fluorescence microscopic images of (a) HPP-1, (b) HPP-2 and (c) HPP-3

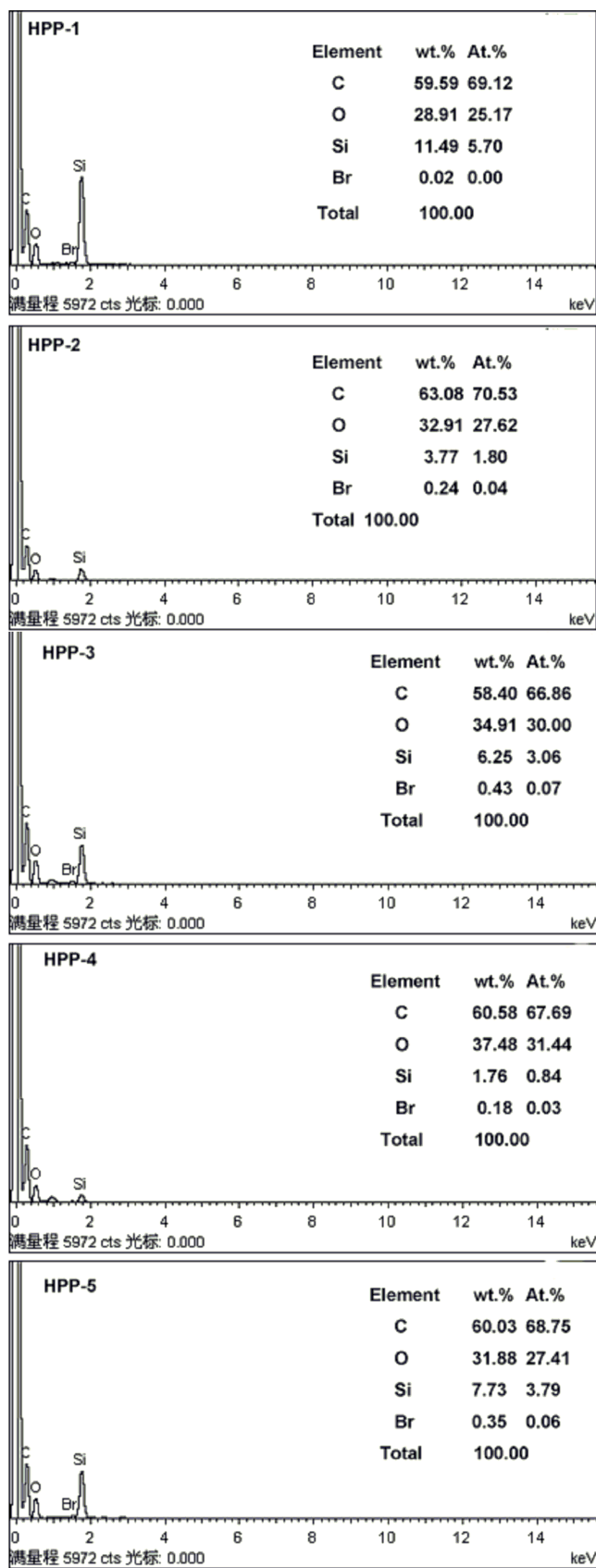


Fig. S1. Energy dispersive spectroscopy of HPP-1 to HPP-5

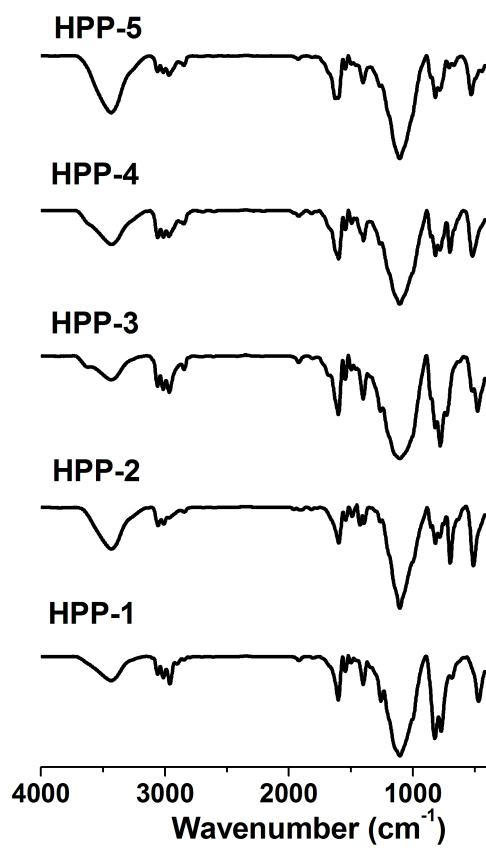


Fig. S2. FT-IR spectrum of HPP-1 to HPP-5

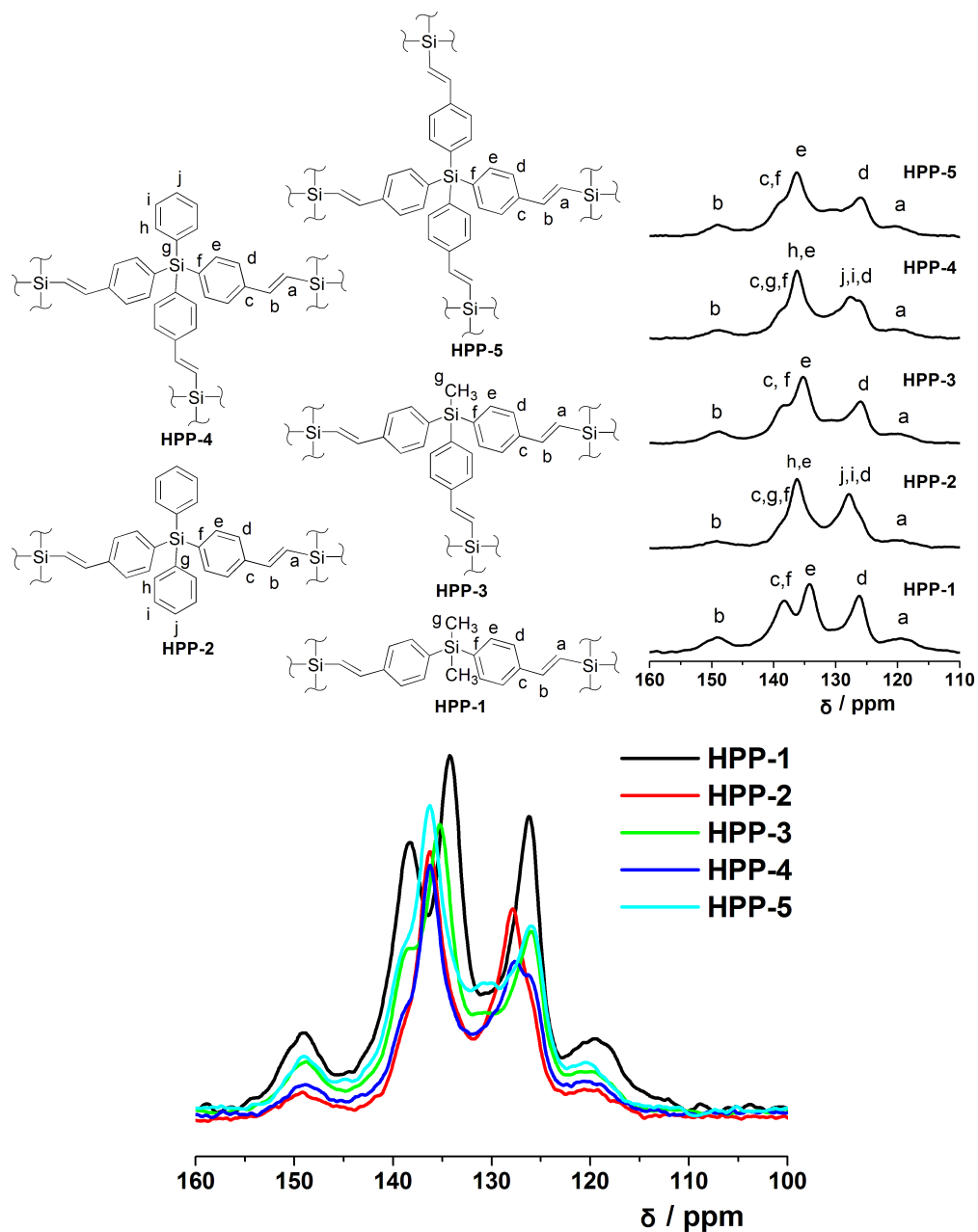


Fig. S3. Solid-state ^{13}C CP/MAS NMR spectra of **HPP-1~HPP-5** at an expanded scale from 100 ppm to 160 ppm

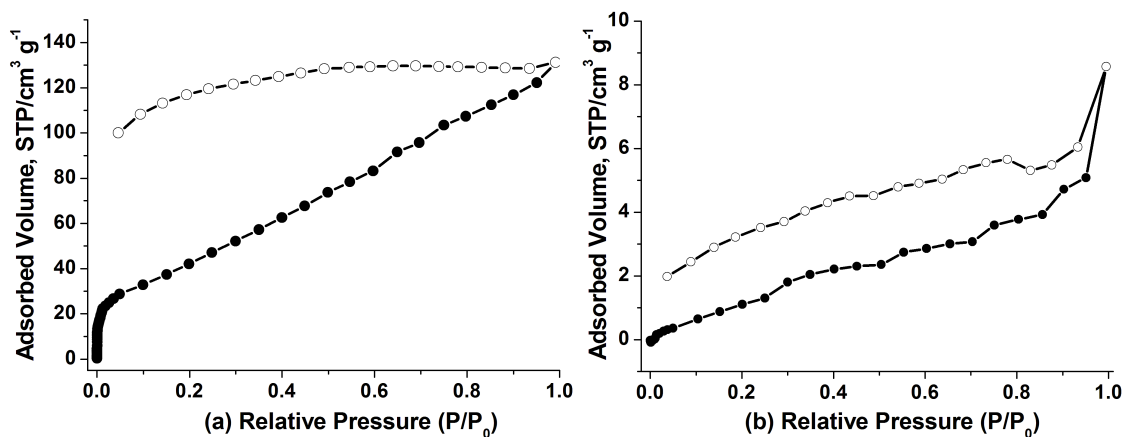


Fig. S4. Nitrogen sorption isotherms of HPP-1 (a) and (b) HPP-2. Filled and empty symbols denote adsorption and desorption branches. The porosity data of HPP-1: $S_{\text{BET}} = 167 \text{ m}^2 \text{ g}^{-1}$,

$$V_{\text{total}} = 0.18 \text{ cm}^3 \text{ g}^{-1}.$$

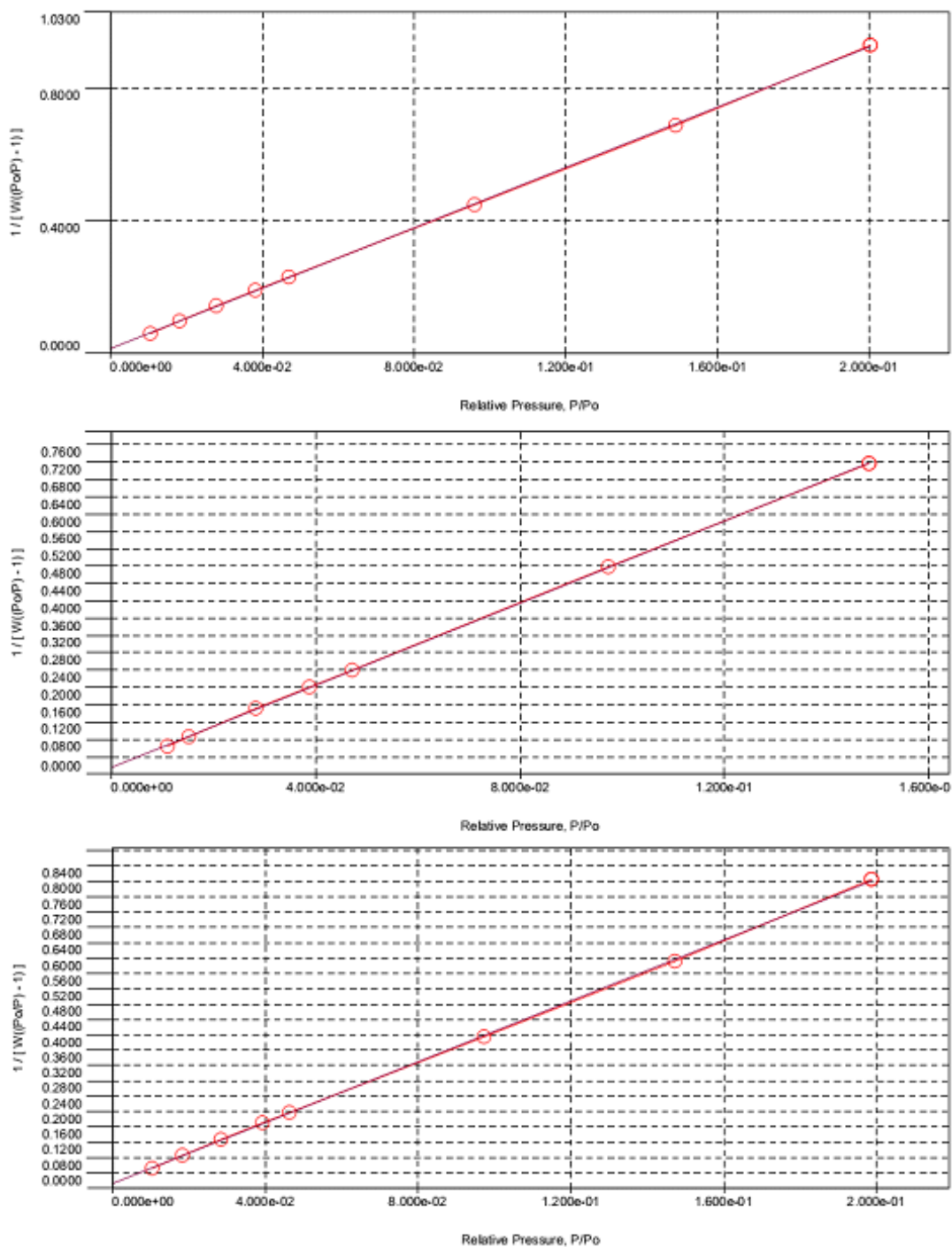


Fig. S5. BET plots of HPP-3 (up, $r = 0.999958$, $C = 290.91$), HPP-4 (middle, $r = 0.999956$, $C = 299.075$) and HPP-5 (bottom, $r = 0.999927$, $C = 298.54$)

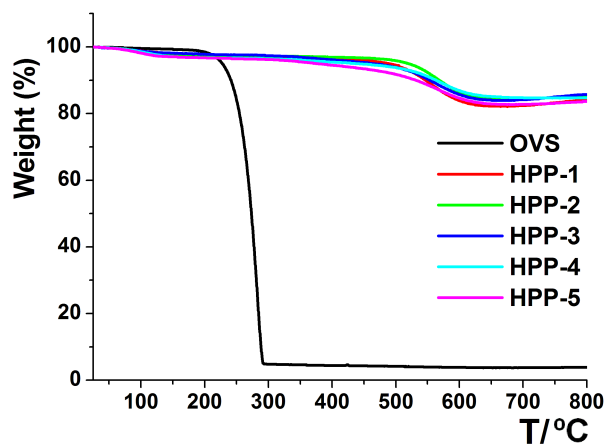


Fig. S6. TGA curves of OVS and HPP-1~HPP-5 under N₂ (10 °C min⁻¹)

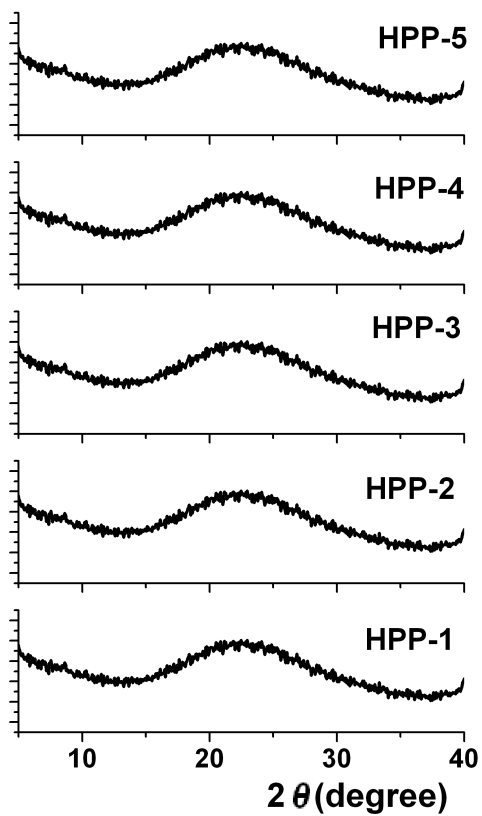


Fig. S7. The XRD pattern of HPP-1 to HPP-5

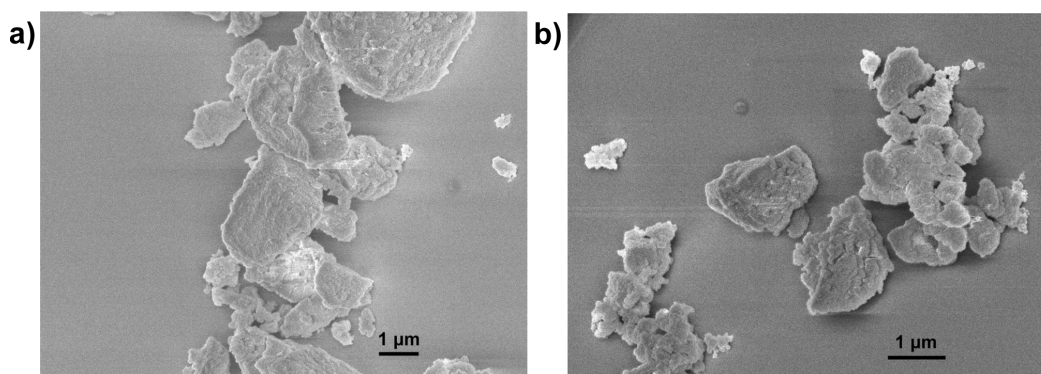


Fig. S8. FE-SEM images of a) HPP-4 and b) HPP-5

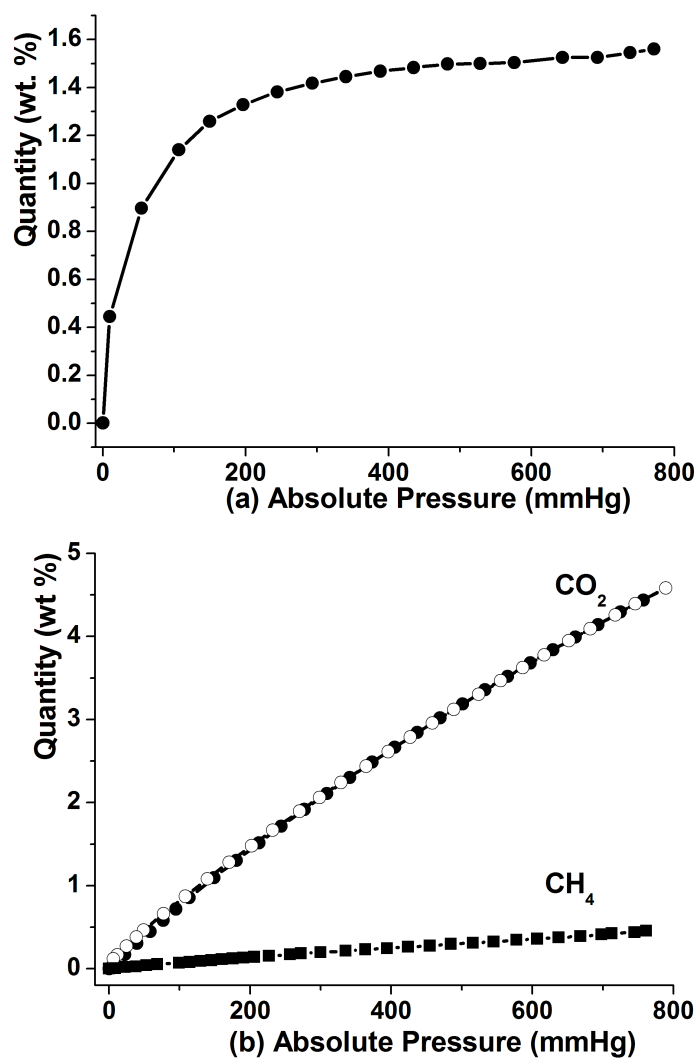


Fig. S9. Gas sorption isotherms of HPP-5. (a) H₂ adsorption isotherm at 77 K. (b) CO₂ adsorption and desorption isotherm, and CH₄ adsorption isotherm at 298 K. Filled and empty symbols denote adsorption and desorption branches, respectively

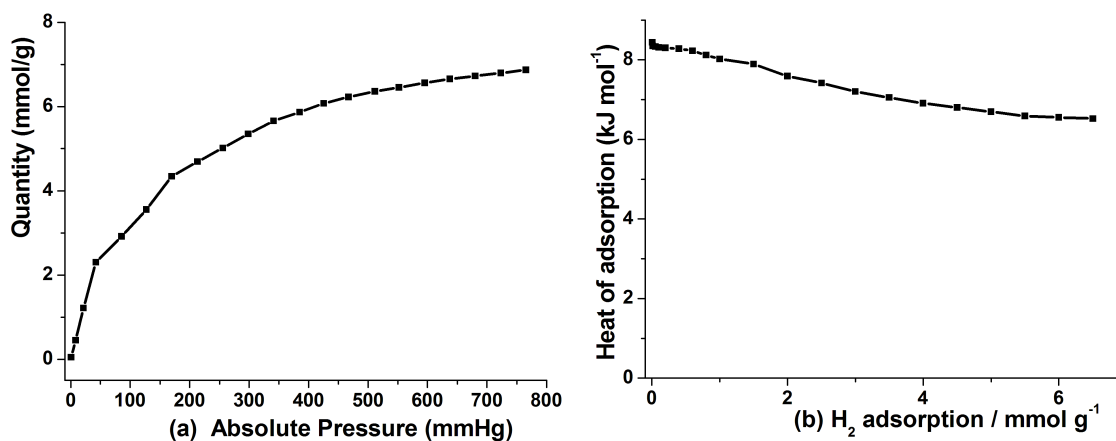


Fig. S10. (a) H₂ adsorption isotherm of HPP-5 at 87 K; (b) Isosteric heats of sorption for H₂ on HPP-5.

Henry's Law selectivity of CO₂ over CH₄ in HPP-5 at 298 K

A nice fitting of CO₂ and CH₄ isotherms has been calculated based on Toth isotherm model.^[1,2]

$$q = q_{sat} \frac{b^{1/t} P}{(1 + b^t)^{1/t}}$$

where q is the uptake in mmol g⁻¹, q_{sat} is the saturation uptake in mmol g⁻¹, P is the pressure in torr, t and b are parameters which are specific for adsorbent pairs.

The Henry law constant K , quantifies the extent of the adsorption of a given adsorbate by a solid. The magnitude of K depends on the properties of both adsorbate and solid. For the Toth isotherm, the Henry law constant is defined by the following equation:

$$K = \lim_{P \rightarrow 0} \left(\frac{dq}{dP} \right) = b^{1/t} q_{sat}$$

Finally, the Henry's Law selectivity $S_{\alpha/\beta}$ of gas α over β is given by the following equation:

$$S_{\alpha/\beta} = \frac{K_{\alpha}}{K_{\beta}}$$

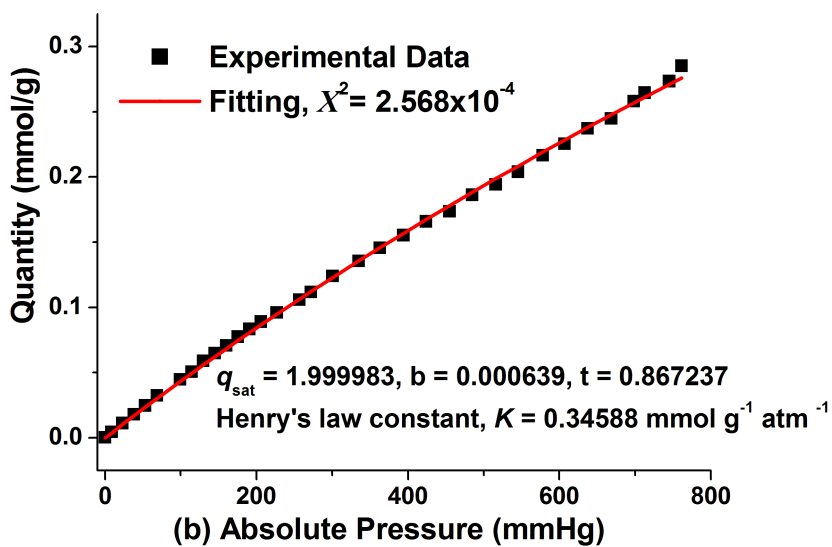
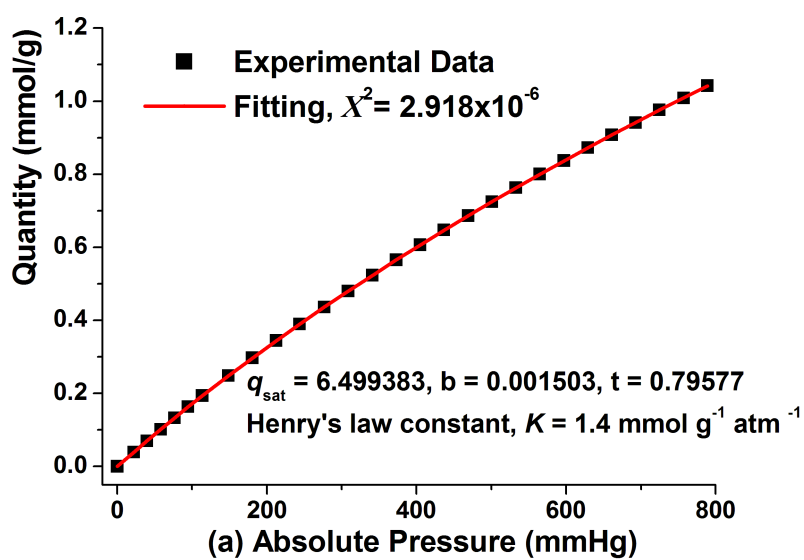


Fig. S11. Toth model fitting of CO₂ (a) and CH₄ (b) adsorption isotherms of HPP-5 at 298 K

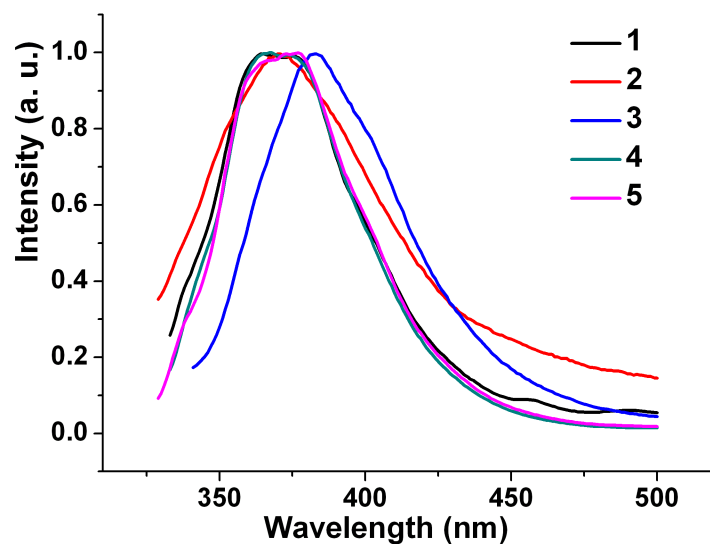


Fig. S12. Fluorescent spectra of monomers, 1~5 in the solid state (excited at 310 nm)

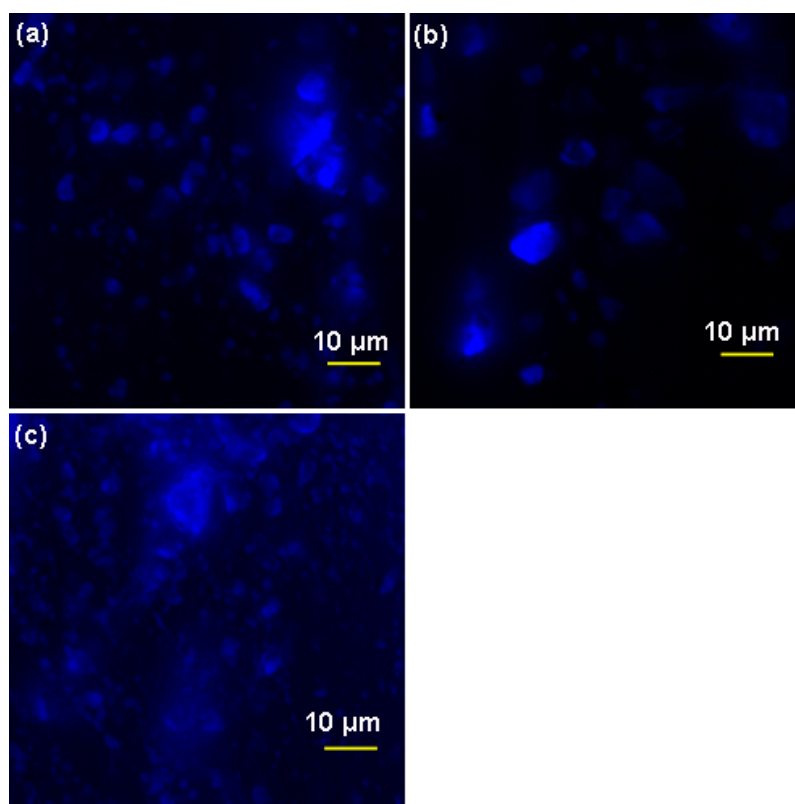


Fig. S13. Fluorescence microscopic images of (a) HPP-1, (b) HPP-2 and (c) HPP-3

References

- [1] E. Neofotistou, C. D. Malliakas, P. N. Trikalitis, *Chem. Eur. J.*, 2009, **15**, 4523–4527.
- [2] B. Wang, A. P. Côté, H. Furukawa, M. O’Keeffe, O. M. Yaghi, *Nature*, 2008, **453**, 207–211.